Thermal Behavior Optimization in Multi-MW Wind Power Converter by Reactive Power Circulation

Zhou, Dao; Blaabjerg, Frede; Lau, Mogens; Tonnes, Michael

Published in:
I E E E Transactions on Industry Applications

DOI (link to publication from Publisher):
10.1109/TIA.2013.2267511

Publication date:
2014

Thermal Behavior Optimization in Multi-MW Wind Power Converter by Reactive Power Circulation

Dao Zhou, *Student Member, IEEE*, Frede Blaabjerg, *Fellow, IEEE*, Mogens Lau and Michael Tonnes

***Abstract* - The influence of actively controlled reactive power on the thermal behavior of multi-MW wind power converter with a Doubly-Fed Induction Generator (DFIG) is investigated. First, the allowable range of internal reactive power circulation is mapped depending on the DC-link voltage as well as the induction generator and power device capacity. Then, the effects of reactive power circulation on current characteristic and thermal distribution of the two-level back-to-back power converter are analyzed and compared. Finally, the thermal-oriented reactive power control method is introduced to the system for the conditions of constant wind speed and during wind gust. It is concluded that the thermal performance will be improved by injecting proper reactive power circulation within the wind turbine system, thereby being able to reduce the thermal cycling and enhance the reliability of the power converter.**

***Index Terms* - Thermal cycling, Doubly-Fed Induction Generator (DFIG), reactive power.**

I. INTRODUCTION

Over last two decades, wind power has expanded greatly, and is forecasted to continue increasing with an average annual growth over 15%. As the power level of single wind turbine is even pushed up to 8 MW (e.g., V164-offshore, Vestas), medium-voltage may become a promising technology in such applications. However, this solution is known to be costly and difficult to repair [1]-[3]. It is still reasonable to consider low-voltage technology in wind power systems with an input and output isolation transformer. Furthermore, wind power converters are being designed for a much-prolonged lifetime of 20-25 years. Industrial experience indicates that dynamic loading, and uncertain and harsh environments are leading to fatigue and a risk of a higher failure rate for power semiconductors. Therefore, more and more efforts are devoted to the thermal behavior and reliability of the power devices in power converters.

Today, it is widely accepted that the reliability of the power semiconductor is closely related to thermal performance, especially the junction temperature fluctuation and the average junction temperature [4]-[13]. Some research has focused on the thermal analysis of wind power converters. In [14], it is noted that the thermal stress of the machine-side converter becomes serious during synchronous operation of the Doubly-Fed Induction Generator (DFIG). The different control schemes of the DFIG system can also affect the power device lifetime [15]. For full-scale power converters, as stated in [16], the thermal performance of the grid-side converter may be improved by circulating proper reactive power among the wind farms.

The scope of this paper, aiming at the DFIG wind turbine system, is first to calculate the allowable reactive power circulation between the back-to-back power converter in different operation modes. Then, the thermal behavior of the back-to-back power converter is investigated under different types of reactive power injection. Finally, a method to improve the lifetime of the power module by proper thermal-oriented control in the conditions of constant wind speed and wind gusts is proposed.

II. BASIC CONCEPT FOR A DFIG SYSTEM

Due to extensive and well-established knowledge, as well as simpler structure and fewer components, the two-level back-to-back voltage source converter is the most attractive solution in the commercial market of wind turbine systems. A popular wind turbine configuration, normally based on a DFIG, is to employ a partial-scale power converter, as shown in Fig. 1. The function of the Rotor-Side Converter (RSC) is not only to transfer the slip active power from/to the grid, but also to provide excitation current for the induction generator, while the Grid-Side Converter (GSC) is designed to keep the DC-link voltage fixed and also supply some of the reactive power required by the grid codes.

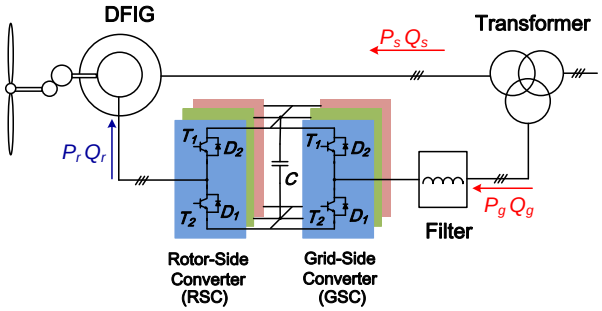

Fig. 1. Typical configuration of a Doubly-Fed Induction Generator wind turbine system.

The parameters of the induction generator and the back-to-back converter used in this paper are summarized in Table I and Table II. The turns ratio between the generator's stator and grid-side converter is assumed 1:1, which implies that the rated stator voltage and the rated grid voltage are the same. Moreover, a common low-voltage power module is selected (1.7 kV/1 kA). Because of the significantly unequal current through the GSC and the RSC, for the sake of similar power device loading, a single power device and two paralleled power devices are the solutions in each GSC and RSC cell, respectively.

TABLE I
PARAMETERS FOR A 2 MW DFIG

Rated power P_m	2 MW
Reactive power range Q_s	-570 kVar ~ +450 kVar
Rated peak stator phase voltage U_{sm}	563 V
Stator/rotor turns ratio k	0.369
Stator inductance L_s	2.95 mH
Rotor inductance L_r	2.97 mH
Magnetizing inductance L_m	2.91 mH

TABLE II
PARAMETERS FOR BACK-TO-BACK POWER CONVERTER

Rated power P_g	330 kW
Rated peak grid phase voltage U_{gm}	563 V
DC-link voltage U_{dc}	1050 V
Filter inductance L_g	0.5 mH
RSC and GSC switching frequency f_s	2 kHz
Power device in each GSC cell	1.7 kV/1 kA
Power device in each RSC cell	1.7 kV/1 kA // 1.7 kV/1 kA

III. EFFECTS OF REACTIVE POWER ON CURRENT CHARACTERISTIC

With the reference direction of the power flow indicated in Fig. 1, both the GSC and the RSC have an ability to control the reactive power. In other words, the system can perform an operation to circulate the reactive power internally without any unexpected power factor distortion to the grid. Although the reactive power flow in the power system will induce voltage drop, additional power dissipation as well as higher capacity of transmission equipment (e.g. cable, transformer, etc), the proper excited power for the induction generator sharing between the stator-side and rotor-side can be used to vary the loss distribution of the back-to-back power converter and even to enhance the power converter efficiency [17].

A. Range of reactive power in Grid-Side Converter

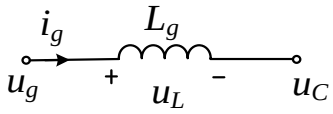

Fig. 2. Simplified single phase diagram of the Grid-Side Converter.

Fig. 2 depicts simplified single phase diagram of the GSC, where L_g represents the filter inductance, U_g represents the grid phase voltage, and U_c represents the output voltage of the GSC. Depending on the definition of power flow, whose direction is consistent with the illustration in Fig. 1, the phasor diagram for the GSC is shown in Fig. 3, in which the capacitive reactive power is applied. Due to the opposite polarity of active power through the GSC between sub-synchronous mode and super-synchronous mode, the active power current reference will be as shown in Fig. 3 (a) and Fig. 3 (b), respectively. Accordingly, if the inductive reactive power is introduced, the phasor diagram can be obtained by rotating the q-axis current 180 degrees.

The analytical formula for the converter output voltage U_c is expressed as,

$$U_C = \sqrt{(U_{gm} + i_{gq} X_g)^2 + (i_{gd} X_g)^2} \le \frac{U_{dc}}{\sqrt{3}} \quad (1)$$

where U_{gm}, U_{dc} denotes rated peak grid phase voltage and DC-link voltage, and X_g denotes filter reactance at 50 Hz, which is also consistent with Table II, i_{gd} and i_{gq} denotes the GSC's peak current in d-axis and q-axis, respectively.

It is evident that whatever the operation mode is, the amplitude of the converter output voltage will be increased if the capacitive reactive power is introduced. Therefore, due to linear modulation, the relationship between the DC-link voltage and output voltage of the GSC is also illustrated in (1).

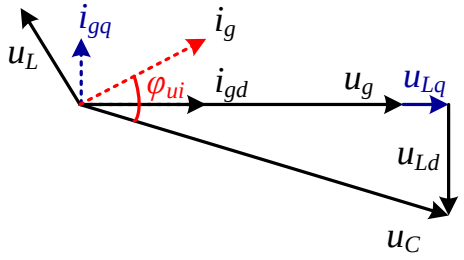

(a) Operating under sub-synchronous mode

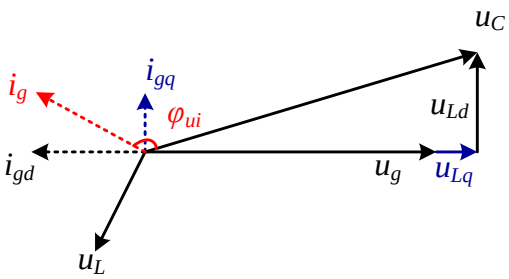

(b) Operating under super-synchronous mode

Fig. 3. Phasor diagram for the Grid-Side Converter (e.g. capacitive reactive power injection).

The other restriction lies in the capacity of the power device/converter,

$$\sqrt{i_{gd}^{\ 2} + i_{gq}^{\ 2}} \le I_m \quad (2)$$

where I_m denotes the peak current of the power module stated in the datasheet.

Furthermore, the induction generator's capacity Q_s must also be taken into account according to Table I,

$$\frac{3}{2} U_{gm} i_{gq} \le Q_s \quad (3)$$

Based on the above mentioned three limitations, the boundary of reactive power can be obtained. Moreover, the power angle is another important indicator for the power loss evaluation, whose feature is described in Fig. 3 as well.

B. Range of reactive power in Rotor-Side Converter

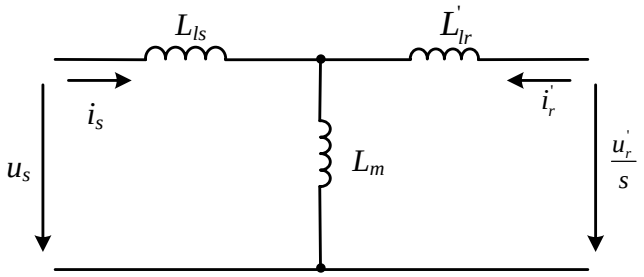

Fig. 4. Equivalent Doubly-Fed Induction Generator circuit diagram in steady-state operation.

Ignoring the stator and rotor resistance, the equivalent DFIG circuit in steady-state operation is shown in Fig. 4, where the parameters of the rotor-side are referred to stator-side by the stator/rotor winding turns ratio *k*. The equations of the rotor current $i_{rd}^{'}$, $i_{rq}^{'}$ and rotor voltage $u_{rd}^{'}$, $u_{rq}^{'}$ under d-q frame in terms of stator current are,

$$\begin{cases} i_{rd}^{'} = -\dfrac{X_s}{X_m} i_{sd} \\ i_{rq}^{'} = -\dfrac{U_{sm}}{X_m} - \dfrac{X_s}{X_m} i_{sq} \end{cases} \tag{4}$$

$$\begin{cases} u_{rd}^{'} = s\left(\dfrac{X_r}{X_m} U_{sm} + \dfrac{\sigma X_r X_s}{X_m} i_{sq}\right) \\ u_{rq}^{'} = -s\dfrac{\sigma X_r X_s}{X_m} i_{sd} \end{cases} \tag{5}$$

where *s* denotes the rotor slip value, σ denotes the leakage factor of the induction generator, U_{sm} denotes rated peak stator phase voltage of the induction generator, X_s, X_r and X_m denotes stator, rotor and magnetizing reactance at 50 Hz, which is consistent with Table I, i_{sd} and i_{sq} denotes the RSC's peak current in d-axis and q-axis, respectively.

If the capacitive reactive power is provided, the phasor diagram for the RSC in the condition of sub-synchronous and super-synchronous mode is depicted in Fig. 5 (a) and (b), respectively. Similar restrictions with the GSC, i.e. the linear modulation, the power device limitation and induction generator capacity,

$$\frac{\sqrt{u_{rd}^{'2} + u_{rq}^{'2}}}{k} \le \frac{U_{dc}}{\sqrt{3}} \tag{6}$$

$$k\sqrt{i_{rd}^{'2} + i_{rq}^{'2}} \le I_m \tag{7}$$

$$-\frac{3}{2} U_{sm} i_{sq} \le Q_s \tag{8}$$

It can be seen that the range of reactive power in the RSC is limited by the induction generator capacity, while in the GSC induction generator capacity affects and DC-link voltage limits the amount of capacitive reactive power.

C. Current characteristic of back-to-back power converter

The current amplitude and the power factor angle of the back-to-back power converter are regarded as two indicators for the power device loading, so it is interesting to investigate the current characteristic based on the reactive power range.

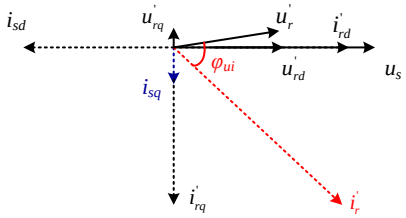

(a) Operating under sub-synchronous mode

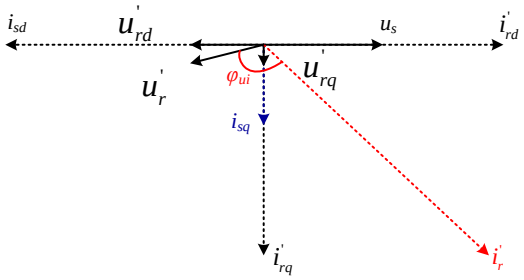

(b) Operating under super-synchronous mode

Fig. 5. Phasor diagram for the Rotor-Side Converter (e.g. capacitive reactive power injection).

If two typical wind speeds of 5.9 m/s and 10.1 m/s are selected for sub-synchronous and super-synchronous operation (these two wind speeds are regarded as two highest probability wind speeds in wind farms [18]), the range of reactive power in the GSC and RSC can be summarized, as listed in Table III. In order not to affect the power factor to the grid, the circulation current is the minimum range of the back-to-back power converter, which is (-0.23, 0.06) from the GSC point of view. As the horizon axis is defined as the reactive power range of the GSC, the injection of additional power not only affects the current amplitude, but also changes the power factor angle φ_{ui}, as shown in Fig. 6.

For the characteristic of current amplitude, regardless of sub-synchronous or super-synchronous operation mode, it is evident that the minimum current appears almost under no reactive power injection for the GSC, while for the RSC the current decreases with larger capacitive reactive power. Unfortunately, the capacitive reactive power is much smaller than the inductive reactive power, which prevents the RSC's current to reach the minimum power losses.

For the characteristic of power factor angle, for the GSC, it is noted that, in response to the additional reactive power injection, unity power factor becomes either leading or lagging power factor. For the RSC, it is noted that the power factor angle presents a tendency to be in phase under sub-synchronous mode or inverse under super-synchronous mode with the increasing capacitive reactive power. However, the phase shift looks insignificant.

TABLE III
RANGE OF THE REACTIVE POWER FOR BACK-TO-BACK POWER CONVERTER

	Sub-synchronous Mode		Super-synchronous Mode	
	Grid-Side Converter	Rotor-Side Converter	Grid-Side Converter	Rotor-Side Converter
Typical wind speed [m/s]	5.9		10.1	
Rated power [p.u.]	0.13		0.65	
Active power current [p.u.]	0.06	0.19	0.11	0.54
Range of reactive power [p.u.]	(-0.23,0.06)	(-0.29,0.23)	(-0.23,0.06)	(-0.29,0.23)

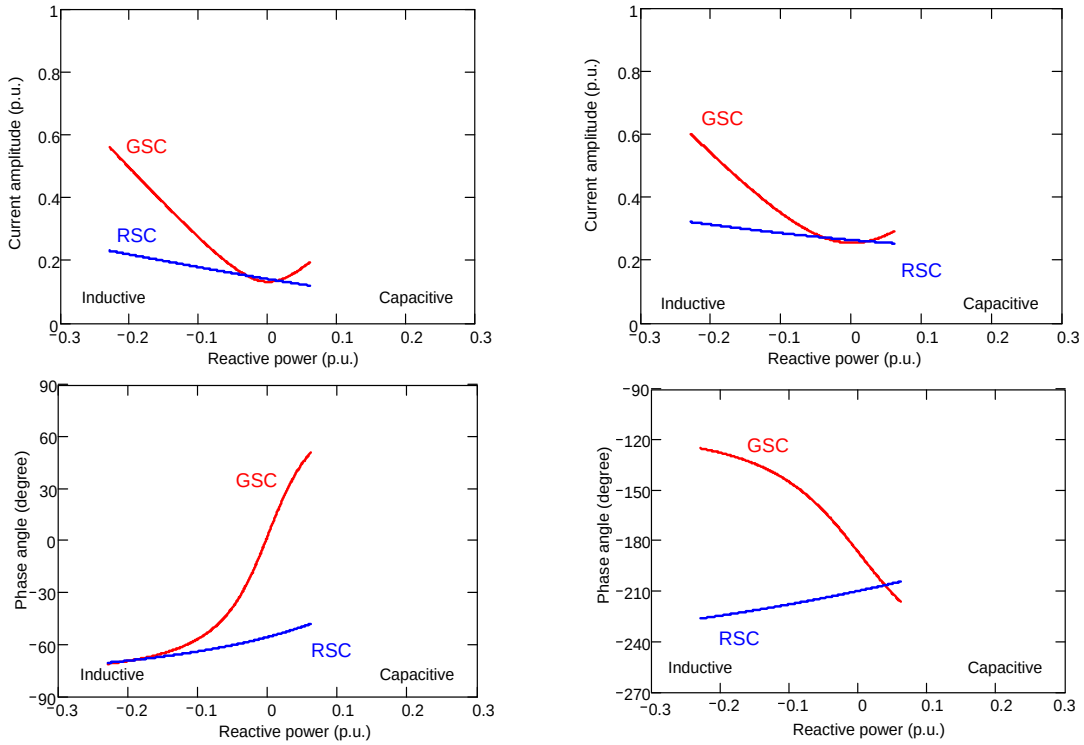

(a) Sub-synchronous mode (wind speed: 5.9 m/s) (b) Super-synchronous mode (wind speed: 10.1 m/s)

Fig. 6. Current characteristic on back-to-back power converter at two different wind speeds.

IV. EFFECTS OF REACTIVE POWER ON THERMAL BEHAVIOR IN POWER DEVICES

Different distribution of the excitation energy between the induction generator's rotor and stator will definitely change the current characteristic of back-to-back power converter. The influence on the thermal performance of the power semiconductor will be investigated in this section.

A. Thermal profile for normal operation

Power losses in power semiconductor can be divided into two categories, conduction losses and switching losses. Based on the loss energy curves provided by the manufacturer, the accumulated power dissipation in every switching cycle can be obtained within one fundamental frequency. Simulations have been realized by PLECS block in Simulink [20].

With the aid of a one-dimensional thermal model mentioned in [19], under normal operation, the relationship between wind speed and junction temperature of each power semiconductor of the back-to-back power converter is as shown in Fig. 7 in terms of junction temperature fluctuation and mean junction temperature. In particular, the wind speed at 8.4 m/s is regarded as the synchronous operation for the DFIG wind turbine system.

It can be seen that when the wind speed increases over the synchronous operation mode of the DFIG, the direction of the power flow in the back-to-back power converter starts to reverse. In the RSC, because the higher power loss changes from the IGBT in sub-synchronous mode to the freewheeling diode in super-synchronous mode, the most thermal stressed power device switches from the IGBT to the freewheeling

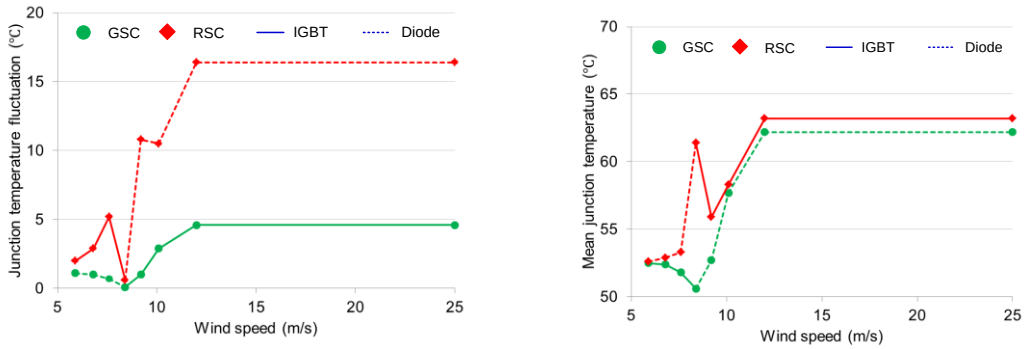

(a) Junction temperature fluctuation (b) Mean junction temperature

Fig. 7. Thermal profile of back-to-back power converter vs. wind speed.

diode, while similarly in the GSC, the most thermal stressed power device changes from the freewheeling diode to the IGBT.

Furthermore, the RSC shows a higher value both in the junction temperature fluctuation and the mean junction temperature throughout the entire wind speed, which indicates the lifetime between the back-to-back power converter will be significantly unbalanced.

B. Thermal profile under reactive power injection

According to the reactive power range circulation within the DFIG system summarized in Table III, the thermal distribution of the GSC and the RSC can be analyzed in the conditions of inductive Q, no Q and capacitive Q. A case study under super-synchronous operation is taken as an example, where the wind speed is selected at 10.1 m/s. The thermal behavior of the GSC is shown in Fig. 8, where the red curve indicates the freewheeling diode and the green curve indicates the IGBT. The thermal behavior of the RSC is depicted in Fig. 9 as well.

Regarding the thermal performance in the GSC as illustrated in Fig. 8, the minimum temperature fluctuation as well as the mean junction temperature appears at no Q, which is consistent with the current characteristics in Fig. 6 (b), while due to a much higher additional reactive power range, the two indicators become more serious in the case of inductive Q compared to capacitive Q.

However, for the RSC, the minimum junction temperature fluctuation as well as the mean junction temperature appears at capacitive Q as shown in Fig. 9. The junction temperature fluctuation and mean junction temperature remain at three conditions almost the same. This is due to the fact that compared to the maximum allowable reactive power – inductive reactive power, the active power reference is dominating as shown in (4). Furthermore, the RSC's two paralleled power modules and the transformation of rotor current in line with the stator/rotor turns ratio result in more stable power device loading, which will lead to nearly a constant junction temperature.

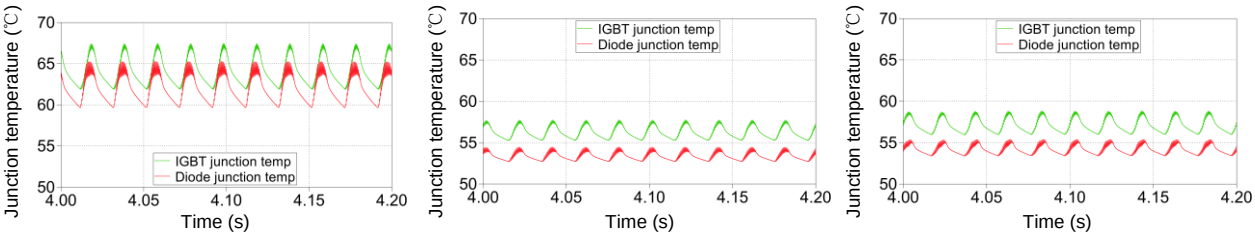

(a) Inductive Q (b) No Q (c) Capacitive Q

Fig. 8. Thermal distribution of GSC at super-synchronous mode (wind speed: 10.1 m/s).

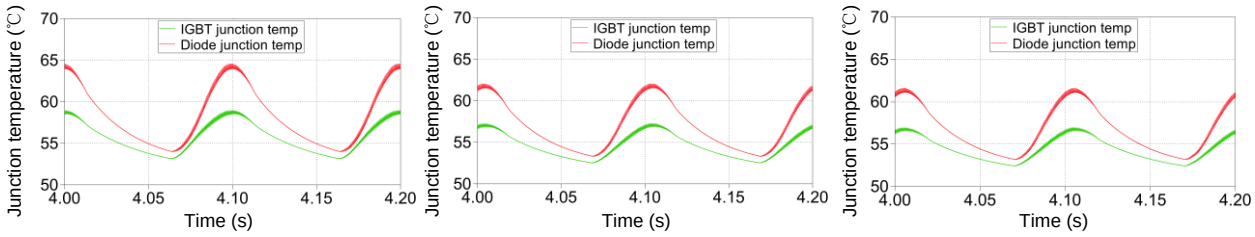

(a) Inductive Q (b) No Q (c) Capacitive Q

Fig. 9. Thermal distribution of Rotor-Side Converter at super-synchronous mode (wind speed: 10.1 m/s).

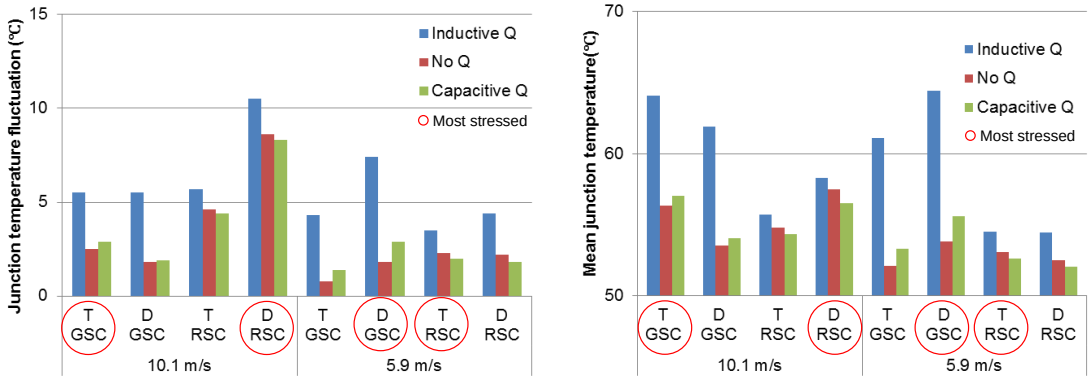

(a) Junction temperature fluctuation (b) Mean junction temperature

Fig. 10. Thermal profile of back-to-back power converter operating under sub-synchronous and super-synchronous mode.

Similarly, if a case of the sub-synchronous mode at wind speed of 5.9 m/s is taken into account, the thermal profile of the back-to-back power converter can be illustrated in Fig. 10 in terms of the junction temperature fluctuation and the mean junction temperature, where the power semiconductor with the red circle is the most stressed.

From the GSC point of view, it can be seen that the least thermal stress appears at no reactive power injection. Moreover, it is noted that the injection of reactive power, especially inductive reactive power could change the junction temperature fluctuation significantly. From the RSC point of view, the additional capacitive reactive power could help to reduce the thermal stress slightly.

V. Thermal Performance Improvement by Reactive Power Control

A. Thermal behavior improvement under constant wind speed

As illustrated in Fig. 7, the RSC is regarded as the most stressed in the back-to-back power converter. Reactive power circulation within the DFIG system may change the thermal distribution both in the GSC and in the RSC, thus it provides the possibility of achieving smaller temperature fluctuation in the most stressed power converter with a proper reactive power under constant wind speed. The control diagram is shown in Fig. 11.

Fig. 12 illustrates the simulation result of operation at the wind speed of 10.1 m/s under super-synchronous mode. The junction temperature flucuation and mean junction temperature of the most stressed power converter could both be decreased, which of course will enhance the power device's lifetime. However, from the GSC point of view, the two reliability indicators both become slightly worse. Therefore, it is a tradeoff as well as a possibility in order to realize similar performance for the back-to-back power converter in respect to the reliability.

B. Thermal behavior improvement under wind gust

As mentioned above, the injection of the reactive power may influence the thermal behavior of the power device. Therefore, it is possible to stabilize the temperature fluctuation under wind gust by proper thermal-oriented reactive power control, as shown in Fig. 13.

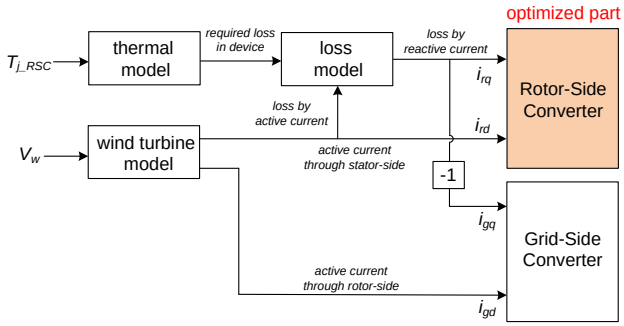

Fig. 11. Thermal-oriented control diagram of the back-to-back power converter under constant wind speed

The typical one-year return period wind gust is defined in IEC, Mexican-hat-like curve [21]. As shown in Fig. 14, the wind speed deceases from an average of 10 m/s to a trough of 8 m/s, increases to a crest of 16 m/s, and returns to 10 m/s within eight seconds, where 8.4 m/s is the synchronous operation wind speed.

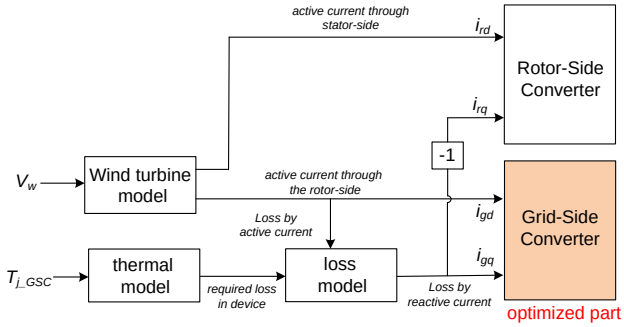

Fig. 13. Thermal-oriented control diagram of back-to-back power converter during wind gust

The thermal cycling of both converters with and without thermal-oriented reactive power control is shown in Fig. 14 (a) and Fig. 14 (b), respectively. It is worth noting that the most stressed power device of the RSC is selected during the synchronous operation point.

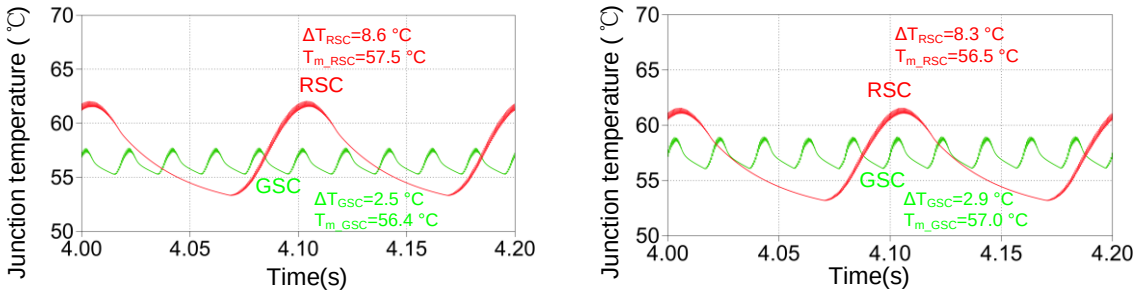

(a) Without thermal-oriented reactive power control (b) With thermal-oriented reactive power control

Fig. 12.Thermal cycling of most stressed power device in both converters under constant wind speed (e.g. super-synchronous mode: wind speed equals 10.1 m/s)

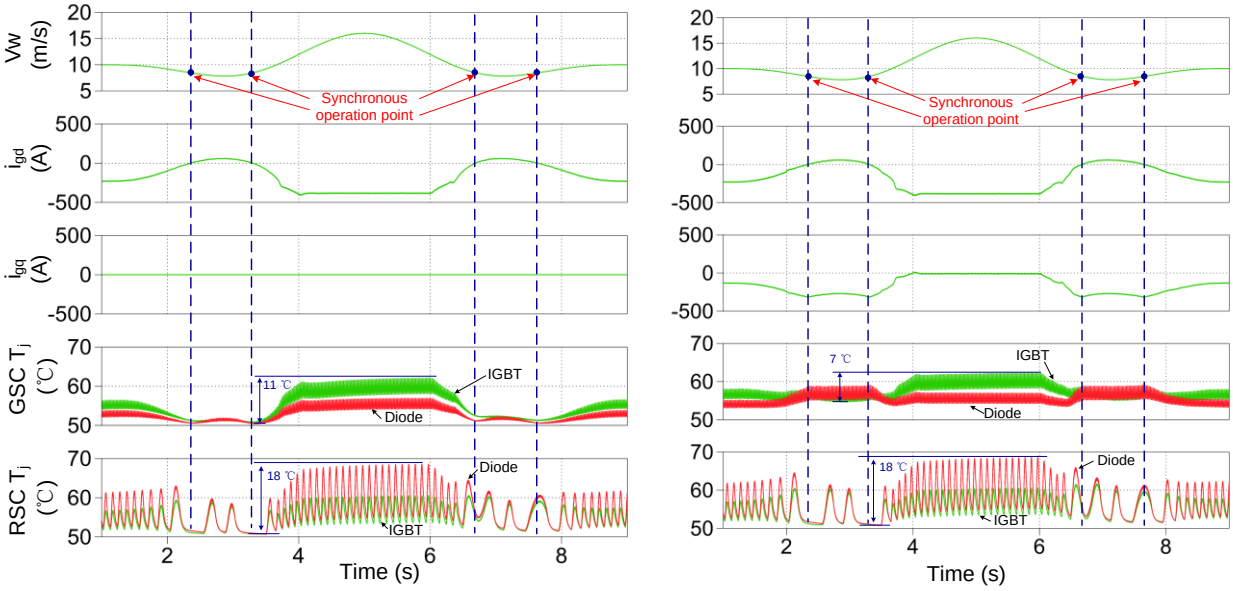

(a) Without thermal-oriented reactive power control (b) With thermal-oriented reactive power control

Fig. 14. Thermal cycling of the back-to-back power converter during wind gusts.

In Fig. 14 (a), the active power reference becomes zero at the synchronous operation point. Moreover, it can be seen that the minimum junction temperature appears at the synchronous operation point and that the maximum junction temperature appears above the rated wind speed. The thermal stress becomes the least serious at synchronous wind speed due to no active power flow in the GSC, while it becomes the most serious at the extreme low frequency current in the RSC.

In Fig. 14 (b), it is noted that by injecting proper thermal-oriented reactive power, the maximum junction temperature fluctuation in the GSC is decreased from 11 ℃ to 7 ℃, due to the introduction of additional thermal-oriented reactive power under small active power in order to actively heat up the device, which will enhance the lifetime of the power converters, while the maximum junction temperature fluctuation in the RSC remains the same 18 ℃ due to the rather higher active power reference in the entire wind speed.

However, when introducing additional reactive power to the wind turbine system in the GSC, the thermal behavior of the diode will become more variable but still has less fluctuation compared to the IGBT. In the RSC, the thermal behavior of the IGBT and the diode are slightly changed.

VI. CONCLUSION

This paper studies the range of reactive power circulation internally between the GSC and the RSC in a DFIG system. It is the GSC that determines the reactive power allowance, which is limited by the DC-link voltage and induction generator capacity. Meanwhile, the range of the capacitive reactive power is much higher than the inductive reactive power.

The additional reactive power will influence the back-to-back power converter's current characteristic and thereby the thermal loading of the power devices. Therefore, it provides the possibility of relieving the thermal cycling either in the GSC or the RSC.

If the wind stays at constant speed, the most stressed power semiconductor of the GSC and the RSC will be more

balanced by the thermal-oriented reactive power injection, which will enhance the temperature loading of the power module.

During a wind gust, the junction temperature fluctuation of the most stressed power semiconductor will be remarkably reduced in the GSC by the thermal-oriented control, which will improve the reliability of the wind power converter. Moreover, the impact on the RSC is not significant.

REFERENCES

[1] Z. Chen, J. M. Guerrero, F. Blaabjerg, "A review of the state of the art of power electronics for wind turbines," *IEEE Trans. on Power Electronics*, vol. 24, no. 8, pp. 1859-1875, Aug. 2009.

[2] F. Blaabjerg, Z. Chen, S.B. Kjaer, "Power electronics as efficient interface in dispersed power generation systems," *IEEE Trans. on Power Electronics*, vol. 19, no. 5, pp. 1184- 1194, Sep. 2004.

[3] M. Liserre, R. Cárdenas, M. Molinas, J. Rodriguez, "Overview of multi-MW wind turbines and wind parks," *IEEE Trans. on Industrial Electronics*, vol. 58, no. 4, pp. 1081-1095, Apr. 2011.

[4] Y. Song, B. Wang, "Survey on reliability of power electronic systems," *IEEE Trans. on Power Electronics*, vol. 28, no. 1, pp. 591-604, Jan. 2013.

[5] A. Bryant, N. Parker-Allotey, D. Hamilton, I. Swan, P.Mawby, T. Ueta, T. Nishijima, K. Hamada, "A fast loss and temperature simulation method for power converters, part I: eletrothermal modeling and validation", *IEEE Trans. on Power Electronics*, vol. 27, no. 1, pp. 248-257, Jan. 2012.

[6] C. Busca, R. Teodorescu, F. Blaabjerg, S. Munk-Nielsen, L. Helle, T. Abeyasekera, P. Rodriguez, "An overview of the reliability prediction related aspects of high power IGBTs in wind power applications," *Microelectronics Reliability*, vol. 51, no. 9-11, pp. 1903-1907, 2011.

[7] B. Lu, S. Sharma, "A literature review of IGBT fault diagnostic and protection methods for power inverters," *IEEE Trans. on Industry Applications*, vol. 45, no. 5, pp. 1770-1777, Sep/Oct. 2009.

[8] D. Hirschmann, D. Tissen, S. Schroder, R.W. De Doncker, "Reliability prediction for inverters in hybrid eletrical vehicles," *IEEE Trans. on Power Electronics*, vol. 22, no. 6, pp. 2511-2517, Nov. 2007.

[9] N. Kaminski, "Load-cycle capability of HiPaks," *ABB Application Note 5SYA 2043-01*, Sep 2004.

[10] O. S. Senturk, L. Helle, S. Munk-Nielsen, P. Rodriguez, R. Teodorescu, "Power capability investigation based on electrothermal models of press-pack IGBT three-level NPC and ANPC VSCs for multi-MW wind turbines," *IEEE Trans. on Power Electronics*, vol. 27, no. 7, pp. 3195-3206, Jul. 2012.

[11] H. Wang, K. Ma, F. Blaabjerg, "Design for reliability of power electronic systems," *in Proc. of IECON 2012*, pp.33-44, 2012.

[12] Y. Avenas, L. Dupont, Z. Khatir, "Temperature measurement of power semiconductor devices by thermo-sensitive electrical parameters – a review", *IEEE Trans. on Power Electronics*, vol. 27, no. 6, pp. 3081-3092, Jun. 2012.

[13] W. Lixiang, J. McGuire, R.A. Lukaszewski, "Analysis of PWM frequency control to improve the lifetime of PWM inverter," *IEEE Trans. on Industry Applications*, vol. 47, no. 2, pp. 922-929, 2011.

[14] J. Jung, W. Hofmann, "Investigation of thermal stress in rotor of doubly-fed induction generator at synchronous operating point," *in Proc. of IEMDC 2011*, pp. 896-901, 2011.

[15] M. Musallam, C.M. Johnson, "Impact of different control schemes on the lifetime consumption of power electronic modules for variable speed wind turbines," *in Proc. of EPE 2011*, pp. 1-9, 2011.

[16] K. Ma, M. Liserre, F. Blaabjerg, "Reactive power influence on the thermal cycling of multi-MW wind power inverter," *IEEE Trans. on Industry Applications*, early access article.

[17] B.C. Rabelo, W. Hofmann, J.L. da Silva, R.G. da Oliveria, S.R. Silva, "Reactive power control design in doubly fed induction generators for wind turbines," *IEEE Trans. on Industrial Electronics*, vol. 56, no. 10, pp. 4154-4162, Oct. 2009.

[18] K. Xie, Z. Jiang, W. Li, "Effect of wind speed on wind turbine power converter reliability," *IEEE Trans. on Energy Conversion*, vol. 27, no. 1, pp. 96-104, Mar. 2012.

[19] D. Zhou, F. Blaabjerg, M. Lau, M. Tonnes, "Thermal analysis of multi-MW two-level wind power converter," *IEEE Trans. on Industrial Electronics*, under review.

[20] User manual of PLECS blockset version 3.2.7 March 2011. (Available: http://www.plexim.com/files/plecsmanual.pdf).

[21] Wind turbines, part 1: Design requirements, IEC 61400-1, 3rd edition, International Electrotechnical Commission, 2005.

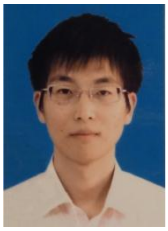

Dao Zhou (S'12) received the B.Sc. in electrical engineering from Beijing Jiaotong University, Beijing, China, in 2007, and the M. Sc. in power electronics from Zhejiang University, Hangzhou, China, in 2010. From 2012, he is pursuing the Ph.D degree in the Department of Energy Technology, Aalborg University, Aalborg, Denmark.

His research interests include two-level power electronics converters and their application in wind power generation systems.

Frede Blaabjerg (S'86-M'88-SM'97-F'03) received the Ph.D. degrees from Aalborg University, Aalborg East, Denmark in 1995.

He was employed at ABB-Scandia, Randers, from 1987-1988. He became Assistant Professor in 1992, Associate Professor in 1996 and full professor in power electronics and drives in 1998. He has been part-time research leader at Research Center Risoe in wind turbines. In 2006-2010 he was dean of the faculty of Engineering, Science and Medicine and became visiting professor at Zhejiang University, China in 2009. His research areas are in power electronics and its applications like wind turbines, PV systems and adjustable speed drives. Since 2006 he has been Editor in Chief of the IEEE Transactions on Power Electronics. He was Distingueshed Lecturer for the IEEE Power Electronics Society 2005-2007 and for IEEE Industry Applications Society from 2010-2011.

Dr. Blaabjerg received the 1995 Angelos Award for his contribution in modulation technique and the Annual Teacher prize at Aalborg University. In 1998 he received the Outstanding Young Power Electronics Engineer Award from the IEEE Power Electronics Society. He has received ten IEEE Prize paper awards and another prize paper award at PELINCEC Poland 2005. He received the IEEE PELS Distingueshed Service Award in 2009 and the EPE-PEMC 2010 Council award.

Mogens Lau (Non-member) received the M.Sc. in power electronics and drives from Aalborg University, Aalborg, Denmark, in 1999. Now he is the R&D manager of Danfoss power stack.

Michael Tonnes (Non-member) received the Ph.D in electrical engineering from Aalborg University, Aalborg, Denmark. Currently he is the senior director of Danfoss power stack at Danfoss Silicon Power GmbH.